Electronic Supplementary Material (ESI) for Physical Chemistry Chemical Physics.

Electronic Supplementary Information:

Theoretical Investigations on Charge Transfer Properties of Thiophene α-Substituted Naphthodithiophene Diimides: Excellent n-Channel and Ambipolar Organic Semiconductors

Li-Fei Ji,[a] Jian-Xun Fan,[a,b] Shou-Feng Zhang,[a] Ai-Min Ren*[a]

a: Laboratory of Theoretical and Computational Chemistry, Institute of Theoretical Chemistry, Jilin University, Changchun, 130023, China

b: College of Chemistry and Environment, Weinan Normal University, Weinan 714000, China

S1. Selection of functional and basis set

To test the reliability of the calculated results, another three functionals including B3PW91, M06-2X and PBE1PBE are chosen to examine if there is any difference from the B3LYP functional. The HOMO/LUMO energies, energy gaps, as well as hole and electron reorganization energies for NDTI are listed in Table S1. It is found that M06-2X tend to underestimate the energy level of HOMO and overestimate the energy level of LUMO and energy gaps compared with the experimental values; and the reorganization energies evaluated by this method are much larger than other methods. While the results obtained by B3PW91, B3LYP, and PBE1PBE methods are similar. The HOMO energy and the energy gap obtained from B3LYP are closer to the experimental values compared with the B3PW91 and PBE1PBE results. The LUMO energy of B3PW91 is closer to exp. On the basis of HOMO energy and the energy gap, B3LYP can be chosen as best functional. On the other hand, B3LYP has been proven suitable to describe the geometric relaxation of charge transfer process for various organic systems so far. So B3LYP functional was selected out for geometry optimizations and frequency calculations in this study.

Table S1. Calculated HOMO/LUMO energies (E_{HOMO}/E_{LUMO}, in eV), energy gaps (Eg, in eV), hole and electron reorganization energies (λ_h/λ_e, in meV) for NDTI by different functional coupled with 6-31G(d,p) basis set.

Methods	E_{HOMO}	E_{LUMO}	Eg	λ_h	λ_e
PBE1PBE	-6.30	-3.45	2.82	134	271
B3LYP	-6.06	-3.48	2.51	140	263
B3PW91	-6.17	-3.60	2.57	134	257
M06-2X	-7.19	-2.78	4.41	206	358
Exp.	-6.10	-4.00	2.10		

Table S2. Calculated HOMO/LUMO energies (E_{HOMO}/E_{LUMO}, in eV) and energy gaps (Eg, in eV) by B3LYP with different basis sets and experimental values for NDTI

Basis sets	E_{HOMO}	E_{LUMO}	Eg
6-31G(d)	-6.06	-3.47	2.59
6-31G(d, p)	-6.06	-3.48	2.58
6-31+G(d)	-6.32	-3.79	2.53
6-31+G(d, p)	-6.33	-3.80	2.53
Exp.	-6.10	-4.00	2.10

Furthermore, in order to investigate the influence of basis set, different basis sets 6-31G(d), 6-31G(d,p), 6-31+G(d), and 6-31+G (d,p) using B3LYP functional were also employed to optimize the molecular geometries of NDTI. The alkyl groups on the nitrogen atoms are simplified as methyl groups. The results show that equilibrium geometries of NDTI at different levels are similar and close to the configuration in crystal. The HOMO/LUMO energies and energy gaps of NDTI at different levels are listed in Table S2. The basis sets without diffusion functions overestimated the energy level of LUMO and energy gap compared with the experimental values; while the basis sets with diffusion functions underestimated HOMO energy.

Considering the computational cost and times, we used B3LYP functional coupled with 6-31G(d,p) basis set to optimize all molecular geometries. Following each optimization, the vibrational frequencies were calculated to make sure stable structures without imaginary vibration frequency. Based on the geometries optimized by B3LYP/6-31G(d,p), B3LYP functional with various basis sets was employed to calculated the HOMO/LUMO energies (E_{HOMO}/E_{LUMO}) of these complexes. The

HOMO/LUMO energies for the complexes studied in this work at different levels are listed in Table S3. It can be found that the values of HOMO and LUMO energies at B3LYP/6-311+G(d,p) level are closest to the experimental values. The results obtained at levels of B3LYP/6-31+G(d,p) and B3LYP/jun-cc-pVDZ are close to each other. In addition, the adiabatic ionization potential IP(a) and adiabatic electron affinity EA(a) of NDI, TDI, NDTI and the derivatives NDTI-X were calculated at the B3LYP/6-31G(d,p) and B3LYP/6-311+G(d,p)//B3LYP/6-31G(d,p) levels and are listed in Table S4. it was found that the effect of the diffusion functions on reorganization energy is negligible. So the 6-311+G(d,p) basis set was employed to characterize the electronic properties of these complexes in our work.

Table S3. Calculated HOMO/LUMO energies (E_{HOMO}/E_{LUMO}, in eV) for NDI, TDI and NDTI-X compounds by B3LYP functional with different basis sets of 6-31G(d,p), 6-31+G(d,p), jun-cc-pVDZ and 6-311+G(d,p) based on the geometries at the B3LYP/6-31G(d,p) levels. And experimental values for some of these compounds are also listed.

Compounds	Exp.		B3LYP/6-311+G(d,p)		B3LYP/6-31+G(d,p)		B3LYP/jun-cc-pVDZ		B3LYP/6-31G(d,p)	
	E_{HOMO}	E_{LUMO}	E_{HOMO}	E_{LUMO}	E_{HOMO}	E_{LUMO}	E_{HOMO}	E_{LUMO}	E_{HOMO}	E_{LUMO}
NDI	-7.1	-3.9	-7.39	-3.82	-7.35	-3.77	-7.35	-3.78	-7.04	-3.41
TDI	-5.96	-4.13	-6.20	-4.11	-6.15	-4.06	-6.16	-4.06	-5.85	-3.73
NDTI	-6.1	-4	-6.37	-3.84	-6.33	-3.79	-6.33	-3.80	-6.06	-3.48
NDTI-F			-6.60	-3.94	-6.55	-3.90	-6.56	-3.90	-6.23	-3.55
NDTI-Cl		-4.1	-6.57	-3.99	-6.53	-3.95	-6.53	-3.95	-6.29	-3.67
NDTI-CN			-7.07	-4.60	-7.03	-4.56	-7.03	-4.56	-6.76	-4.25
NDTI-B	-5.8	-4.1	-6.06	-3.71	-6.02	-3.67	-6.03	-3.67	-5.75	-3.36
NDTI-T			-5.92	-3.70	-5.87	-3.66	-5.88	-3.67	-5.60	-3.36
NDTI-BT	-5.9	-4.1	-5.94	-3.77	-5.90	-3.73	-5.91	-3.74	-5.63	-3.43
NDTI-NT	-5.8	-4.2	-5.76	-3.81	-5.71	-3.76	-5.73	-3.77	-5.46	-3.47

Table S4. The adiabatic ionization potentials and electron affinities (IP(a)/EA(a), in eV), and the hole and electron reorganization energies (λ_h/λ_e, in meV) calculated by adiabatic potential surfaces (AP) at B3LYP/6-31G(d,p) and B3LYP/6-311+G(d,p)//B3LYP/6-31G(d,p) levels for NDI, TDI and NDTI-X compounds.

Compounds	B3LYP/6-311+G(d,p)				B3LYP/6-31G(d,p)			
	IP(a)	EA(a)	λ_h(AP)	λ_e(AP)	IP(a)	EA(a)	λ_h(AP)	λ_e(AP)
NDI	8.82	2.49	202	334	8.52	2.04	202	335
TDI	7.39	2.92	136	273	7.11	2.53	136	274
NDTI	7.61	2.63	136	261	7.36	2.24	140	263
NDTI-F	7.81	2.75	233	295	7.48	2.33	238	294
NDTI-Cl	7.72	2.83	209	260	7.49	2.49	209	261
NDTI-CN	8.25	3.45	121	221	7.99	3.08	123	222
NDTI-B	7.03	2.67	236	210	6.74	2.30	239	210
NDTI-T	6.87	2.68	235	189	6.59	2.31	236	190
NDTI-BT	6.80	2.81	203	177	6.52	2.46	204	177
NDTI-NT	6.56	2.90	110	165	6.28	2.55	112	165

Table S5. The π-π Stacking Motifs in C8-NDTI and C8-NDTI-Cl Crystals: Interplanar Distance d (Å), Displacement along Short and Long Axis (Å), and Electron Transfer Integral (meV).

	Crystalline motif	d (Å)	Displacement		V_e (meV)
			Short axis (Å)	Long axis (Å)	
C8-NDTI	slipped π-π stacking	3.40	0.614	3.734	82.1
C8-NDTI-Cl	slipped π-π stacking	3.48	0.898	4.011	120.1

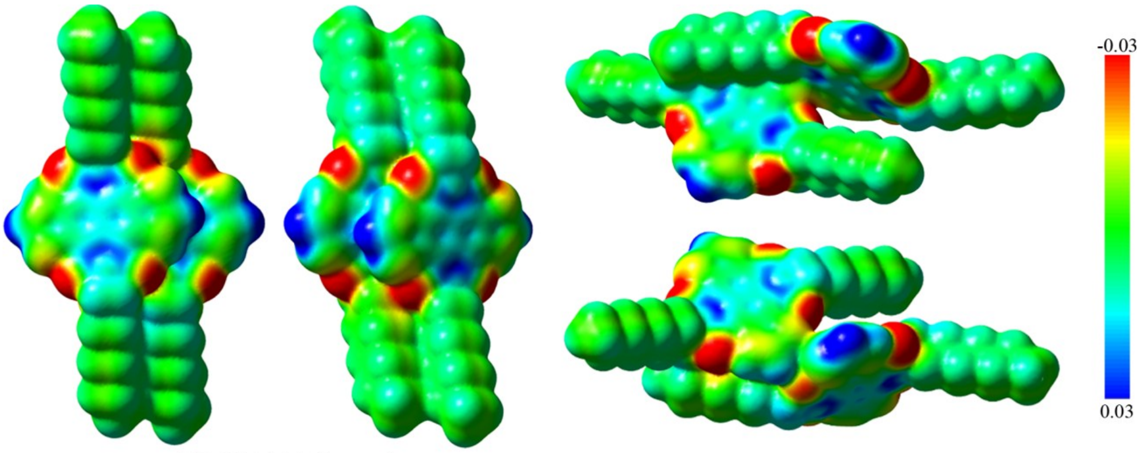

C8-NDTI-dimer1 C8-NDTI-dimer2

Fig. S1. Molecular surface electrostatic potential of dimers of C8-NDTI, computed on the 0.001 a.u. contour of the electronic density by B3LYP/6-31g(d, p) method.

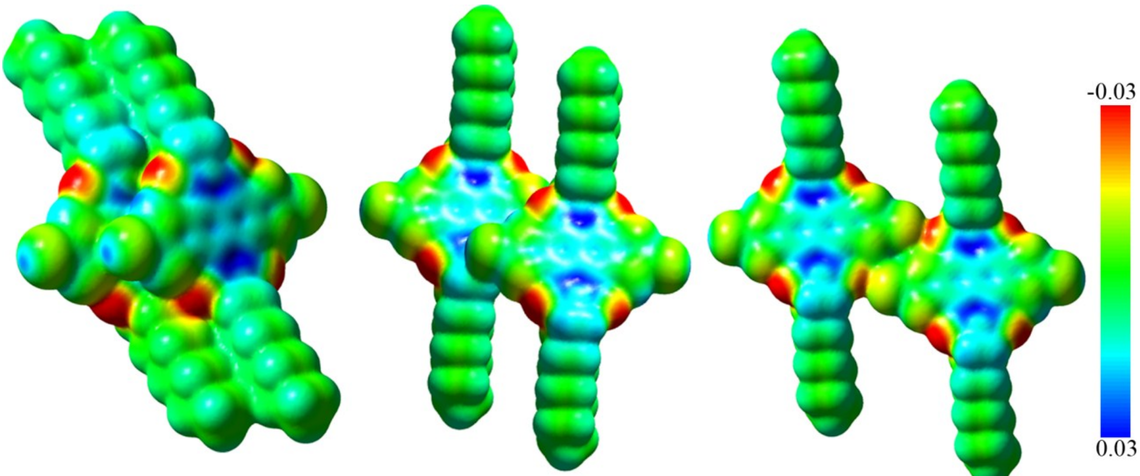

C8-NDTI-Cl-dimer1 C8-NDTI-Cl-dimer2 C8-NDTI-Cl-dimer3

Fig. S2. Molecular surface electrostatic potential of dimers of C8-NDTI-Cl, computed on the 0.001 a.u. contour of the electronic density by B3LYP/6-31g(d, p) method.

a) C8-NDTI-Cl-dimer1

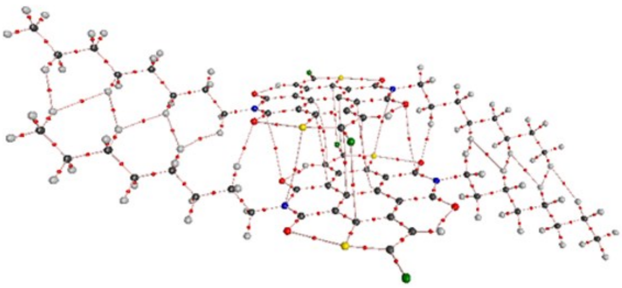

b) C8-NDTI-Cl-dimer2

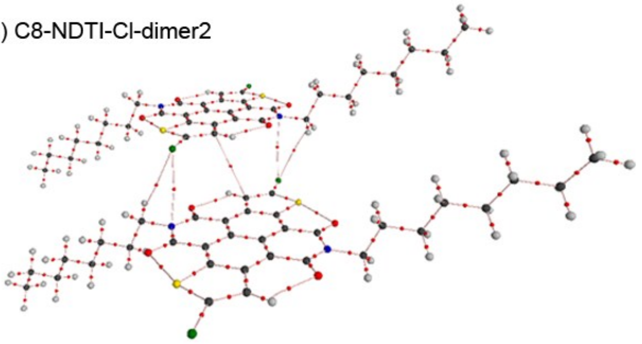

c) C8-NDTI-Cl-dimer3

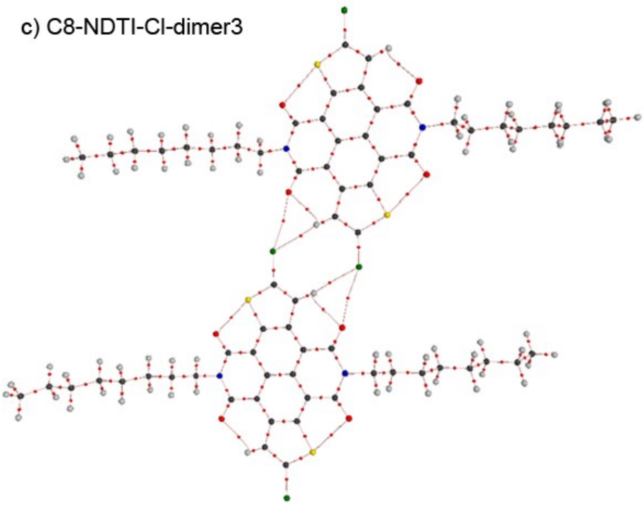

Figure S3. Electron density molecular graphs for a) C8-NDTI-Cl-dimer1, b) C8-NDTI-Cl-dimer2 and c) C8-NDTI-Cl-dimer3, indicating the intermolecular interactions. The red dots represent the location of the bond critical points of the electron density, and the lines connecting the atoms indicate the bond paths.

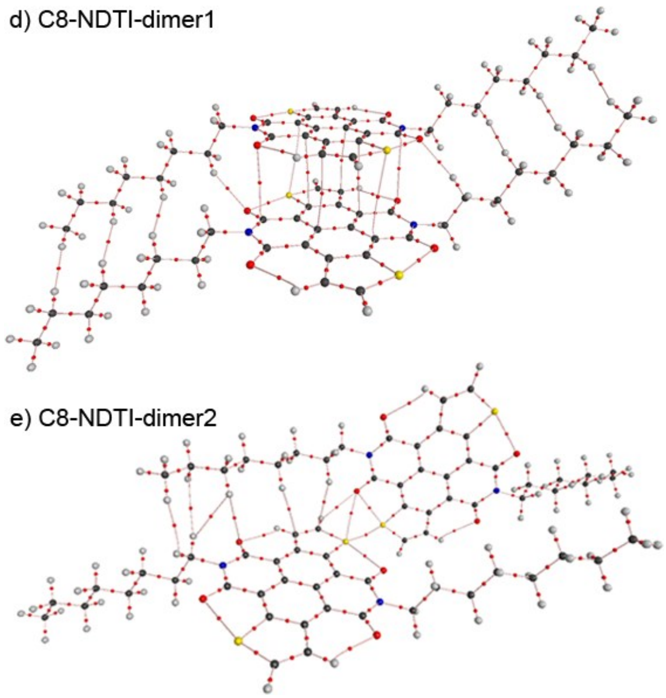

Figure S4. Electron density molecular graphs for d) C8-NDTI-dimer1 and e) C8-NDTI-dimer2/3, indicating the intermolecular interactions. The red dots represent the location of the bond critical points of the electron density, and the lines connecting the atoms indicate the bond paths.

Table S6. Electron density ρ(r) and its Laplacian $\nabla^2\rho(r)$ at the intermolecular bond critical points (BCPs) of C8-NDTI dimer2/3 and C8-NDTI-Cl dimer3. Wave functions are calculated at B3LYP/6-31G(d,p) level.

Bonds	Bond length/Å	ρ (r)	$\nabla^2\rho$ (r)
C8-NDTI dimer2/3			
C–S···S–C	3.728	0.0052	0.0717
C=O···H–C_{sp2}	2.438	0.0101	0.0412
C=O···S–C	3.206	0.0078	0.0298
C_{sp3}–H···π	2.759	0.0065	0.0208
C8-NDTI-Cl dimer3			
C=O···H–C_{sp2}	2.244	0.0176	0.0279
C=O···Cl–C_{sp2}	3.165	0.0064	0.0684
C–Cl···H–C_{sp2}	2.683	0.0086	0.0309

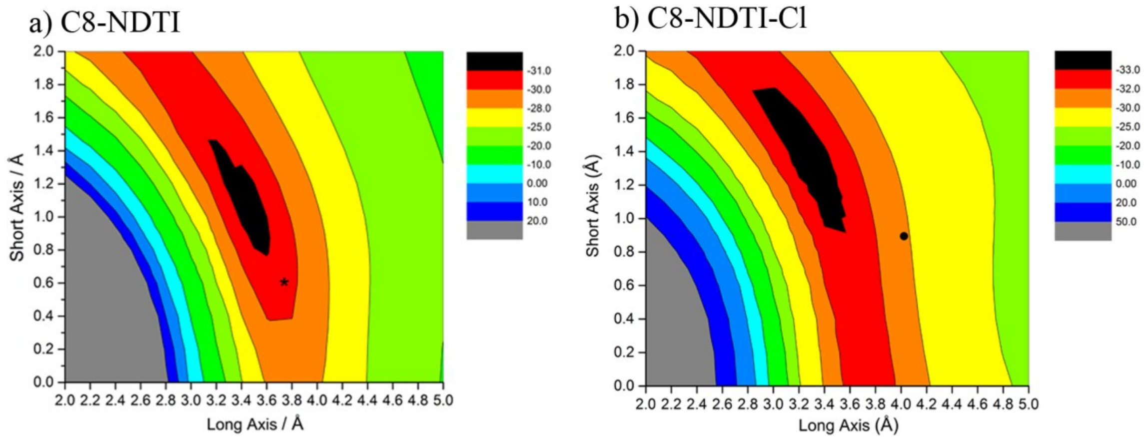

Figure S5. Evolution of the intermolecular interaction energies for (a) an cofacial C8-NDTI dimer, with 3.40 Å interplanar distance and (b) an cofacial C8-NDTI-Cl dimer with 3.48 Å interplanar distance as a function of the long and short axes shifts (Å). Each scanning step is set to be 0.2 Å. The interaction energies were estimated at B3LYP-D3(BJ)/6-31G(d,p) level with BSSE correction. (The face-to-face stacking D1 structures for C8-NDTI and C8-NDTI-Cl in crystal are labeled as black asterisk and dot)

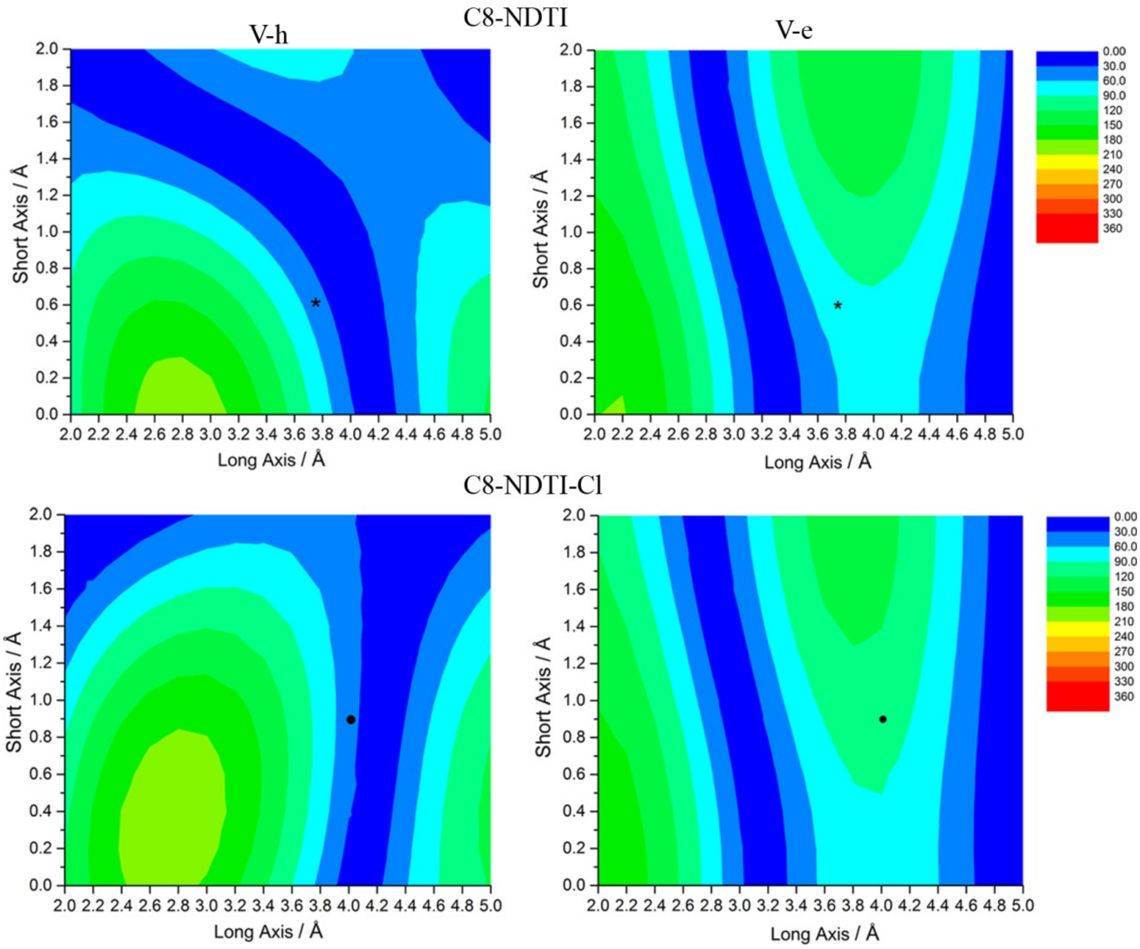

Figure S6. Hole (the left) and electron (the right) transfer integrals (in meV) as a function of displacements along short and long axes. (The face-to-face stacking D1 structures for C8-NDTI and C8-NDTI-Cl in crystal are labeled as black asterisk and dot)